

# Transport of Arylsulfatase A across the Blood-Brain Barrier *in Vitro*\*

Received for publication, September 28, 2010, and in revised form, March 25, 2011. Published, JBC Papers in Press, March 28, 2011, DOI 10.1074/jbc.M110.189381

Frank Matthes<sup>‡1</sup>, Philipp Wölte<sup>§1</sup>, Annika Böckenhoff<sup>‡</sup>, Sabine Hüwel<sup>§</sup>, Mareike Schulz<sup>§</sup>, Pia Hyden<sup>¶</sup>, Jens Fogh<sup>¶</sup>, Volkmar Gieselmann<sup>‡</sup>, Hans-Joachim Galla<sup>§</sup>, and Ulrich Matzner<sup>‡2</sup>

From the <sup>‡</sup>Rheinische Friedrich-Wilhelms Universität, Institut für Biochemie und Molekularbiologie, D-53115 Bonn, Germany, <sup>§</sup>Westfälische Wilhelms-Universität, Institut für Biochemie, D-48149 Münster, Germany and <sup>¶</sup>Zymerex A/S, DK-3400 Hillerød, Denmark

Enzyme replacement therapy is an option to treat lysosomal storage diseases caused by functional deficiencies of lysosomal hydrolases as intravenous injection of therapeutic enzymes can correct the catabolic defect within many organ systems. However, beneficial effects on central nervous system manifestations are very limited because the blood-brain barrier (BBB) prevents the transfer of enzyme from the circulation to the brain parenchyma. Preclinical studies in mouse models of metachromatic leukodystrophy, however, showed that arylsulfatase A (ASA) is able to cross the BBB to some extent, thus reducing lysosomal storage in brain microglial cells. The present study aims to investigate the routing of ASA across the BBB and to improve the transfer *in vitro* using a well established cell culture model consisting of primary porcine brain capillary endothelial cells cultured on Transwell filter inserts. Passive apical-to-basolateral ASA transfer was observed, which was not saturable up to high ASA concentrations. No active transport could be determined. The passive transendothelial transfer was, however, charge-dependent as reduced concentrations of negatively charged monosaccharides in the *N*-glycans of ASA or the addition of polycations increased basolateral ASA levels. Adsorptive transcytosis is therefore considered to be the major transport pathway. Partial inhibition of the transcellular ASA transfer by mannose 6-phosphate indicated a second route depending on the insulin-like growth factor II/mannose 6-phosphate receptor, MPR300. We conclude that cationization of ASA and an increase of the mannose 6-phosphate content of the enzyme may promote blood-to-brain transfer of ASA, thus leading to an improved therapeutic efficacy of enzyme replacement therapy behind the BBB.

Lysosomal storage diseases (LSDs)<sup>3</sup> are a group of ~50 inherited metabolic disorders that result from defects of the lyso-

somal function leading to intralysosomal accumulation of undegraded macromolecules (1). Most LSDs result from functional deficiencies of lysosomal hydrolases involved in the degradation of glycosaminoglycans, sphingolipids, or glycoproteins. The clinical picture of the diseases is diverse. Most forms are progressive and severe multi-systemic diseases that affect the central nervous system and lead to premature death. Although individually rare, the LSDs have a combined prevalence of ~1/8000 live births, making this disease group a major challenge for the health care system (2). Mouse models with various deficiencies for individual lysosomal hydrolases have been utilized to assess the therapeutic potential of enzyme replacement therapy (ERT) (3, 4). The concept of ERT is based on repeated intravenous injection of the corresponding active enzyme to replace the defective one.

Most lysosomal enzymes carry mannose 6-phosphate (Man-6-P) residues, a specific marker that enables their binding to cellular mannose 6-phosphate receptors (MPRs) (5). Binding to MPRs localized to the trans-Golgi network separates newly synthesized lysosomal enzymes from the secretory route and targets them to the endosomal/lysosomal compartment. Importantly, one of the two known MPRs, the insulin-like growth factor II/mannose 6-phosphate receptor, MPR300, also cycles to the plasma membrane where it efficiently internalizes exogenous lysosomal enzymes with Man-6-P residues. The endocytic pathway provides the rationale for ERT as the lysosomally delivered enzyme can substitute for its defective counterpart and degrade the accumulated substrate(s). Almost 20 years of clinical experience indicate that ERT is a safe and effective treatment for a number of LSDs (3, 4). There also is a general consensus that ERT is inappropriate to treat the central nervous system manifestation of LSDs because no beneficial responses of brain and spinal cord have been reported. The lack of central nervous system improvement was ascribed to the blood-brain barrier (BBB), which forestalls transfer of lysosomal enzymes from the circulation to the brain parenchyma.

Surprisingly, ERT of a mouse model of metachromatic leukodystrophy (6) challenged this view as treatment of 1-year-old animals reduced lysosomal storage in brain and spinal cord by up to 34 and 45%, respectively (7, 8). Capillary depletion indicated transendothelial transfer of small, albeit significant amounts of the injected enzyme, recombinant human arylsulfatase A (rhASA), across the BBB.<sup>4</sup> To identify the transendothelial transfer routes, which allow and regulate the trespass of

\* This work was supported by research grants from the "Eva Luise und Horst Köhler Stiftung für Menschen mit Seltenen Erkrankungen," Germany, and the International Graduate School Biotech-Pharma of North-Rhine Westphalia, Germany.

<sup>1</sup> Both authors contributed equally to this work.

<sup>2</sup> To whom correspondence should be addressed: Nussallee 11, D-53115 Bonn, Germany. Tel.: 49-228-735046; Fax: 49-228-732416; E-mail: matzner@ibmb.uni-bonn.de.

<sup>3</sup> The abbreviations used are: LSD, lysosomal storage disease; ASA, arylsulfatase A; BBB, blood-brain barrier; BHK, baby hamster kidney; CHO-S, chinese hamster ovary suspension; ERT, enzyme replacement therapy; Man-6-P, mannose 6-phosphate; MPR, mannose 6-phosphate receptor; PBCEC, porcine brain capillary endothelial cell; rhASA, recombinant human ASA; TEER, transendothelial electrical resistance; Endo H, endoglycosidase H.

<sup>4</sup> U. Matzner, unpublished results.

## ASA Transport across the BBB

rhASA across the BBB, we analyzed the apical-to-basolateral transfer of rhASA in a porcine cell culture model of the BBB. Our experiments led to the identification of pathways and of factors that increase transfer rates. Our findings may be exploited in future ERT trials to improve the supply of the central nervous system with therapeutic enzyme not only in metachromatic leukodystrophy but possibly also in other LSDs.

### EXPERIMENTAL PROCEDURES

#### BBB Cell Culture Model

Primary porcine brain capillary endothelial cells (PBCECs) from ~6-month-old pigs were cultured on rat tail collagen-coated filters with microporous polycarbonate membranes (Costar® Transwell™, Corning, Wiesbaden, Germany) essentially as described (9, 10). After 48 h, the plating medium was replaced by serum-free culture medium without L-cysteine, L-methionine, and phenol red but containing 550 nM hydrocortisone (Sigma-Aldrich). The medium volumes were 0.5 ml (apical) and 1.0 ml (basolateral), respectively. After differentiation (48 h) to monolayers displaying high transendothelial electrical resistances (TEERs), ASA transfer experiments were performed.

#### ASA Transfer Experiments

rhASA (57 kDa) was isolated from secretions of stably transfected CHO-S cells overexpressing the wild-type human ASA using combinations of ion exchange, hydrophobic, and size exclusion chromatography (11). Unless otherwise indicated, rhASA was added at a final concentration of 0.1 mg/ml to the apical medium of the cell culture model. This concentration was chosen because it resembles the minimum plasma peak concentration of rhASA that causes corrective effects in the brain of metachromatic leukodystrophy mice treated by ERT (7). Apical, cell-associated, and basolateral rhASA levels were measured 24 h after addition of rhASA by ELISA. In initial experiments, only ~30% of the input rhASA could be recovered from the system. BSA (3 mg/ml; Sigma-Aldrich) increased the recovery to 65–75% and therefore was added routinely to the apical and basolateral medium during transfer studies. Transfer rates were calculated by relating the basolateral amount of rhASA to the apical amount of rhASA measured at termination. During the transfer experiment, barrier tightness was monitored by continuous TEER measurements using the cell-Zscope® device (nanoAnalytics, Münster, Germany). Wells in which any of the TEER values dropped below 600 ohms  $\times$  cm<sup>2</sup> were excluded from the statistical evaluation of the experiment. TEER measurements were not possible during the final harvesting of media. To identify wells in which apical medium leaked into the basolateral medium during harvesting, apical media were supplemented with 0.25 mg/ml FITC-labeled dextran (molecular mass of 70 kDa, Sigma-Aldrich) at  $t_0$ . The concentration of FITC-labeled dextran was determined fluorometrically (excitation, 485 nm; emission, 535 nm) in the collected basolateral media using a Mithras LB 940 microplate reader (Berthold Technologies, Bad Wildbad, Germany). Wells in which the terminal basolateral FITC-dextran concentration exceeded 125 ng/ml, indicating that the cell layer had been disrupted during harvesting were excluded from analysis.

#### Cellular Uptake Measurements

Filters with PBCEC monolayers were cut out of the Transwell filters, washed three times with 500 ml 1 $\times$  PBS each (pH 7.4) and lysed in homogenization buffer (1 $\times$  TBS (pH 7.4) 0.5% Triton N-101). The rhASA in the homogenate was determined by ELISA and defined as cell-associated rhASA. For the discrimination of surface-bound and intracellular rhASA, filters were additionally washed with 50 mM glycine, 150 mM NaCl (pH 3.0), before homogenization. Then, the rhASA levels of the cell homogenate (intracellular rhASA) and acid-wash fraction (surface-bound rhASA) was determined by ELISA.

#### Immunocytochemistry

PBCECs cultured on Transwell filters and cryosections through forebrain specimen of ~6-month-old pigs were immunostained as described (12). Rabbit anti ZO-1 (Zytomed, Berlin, Germany, 2.5  $\mu$ g/ml), mouse anti PECAM1 (CD31; Novus Biologicals, Littleton; 1:100), and rabbit anti-MPR300 (kindly provided by S. Höning (Cologne, Germany; 1:100)) were used as primary antibodies. The secondary antibodies Alexa Fluor® 488-conjugated goat anti-rabbit IgG, Alexa Fluor® 488-conjugated goat anti-mouse IgG, and Alexa Fluor® 568-conjugated goat anti-rabbit IgG were from Invitrogen and used in 1:1000 dilutions. Filters with immunostained cells were cut out of the plastic insert. Filters and sections were mounted in Aqua Poly/Mount (Polysciences) and analyzed by confocal laser scanning microscopy with a Leica TCS SL microscope (Leica Microsystems, Wetzlar, Germany).

#### Recombinant Lysosomal Enzymes

Recombinant human  $\alpha$ -galactosidase A was provided kindly by Shire HGT. ASA activity was measured with the artificial substrate *p*-nitrocatechol sulfate (13). ASA and protein concentrations were determined by an indirect sandwich ELISA specific for human ASA (14) and the Bio-Rad DC assay, respectively. For one experiment, rhASA was fractionated by Source 30Q anion exchange chromatography (GE Healthcare) using a linear gradient of 60–500 mM NaCl in 10 mM sodium phosphate (pH 7.5) for elution (method available in patent application 20080003211 on the FreshPatents website). The monosaccharide composition of *N*-glycans released from the different rhASA fractions was analyzed as described (11).

#### Enzymatic Modifications of rhASA Deglycosylation

*N*-glycans were cleaved from rhASA by endoglycosidase H (Endo H) treatment. One milligram of rhASA was reacted with 6 milliunits of Endo H<sub>f</sub> (New England Biolabs) in a total volume of 1 ml in the supplied reaction buffer for 24 h at 37 °C. Deglycosylation was controlled by the electrophoretic size shift in SDS-PAGE. Endo H<sub>f</sub> treatment removed >95% of the *N*-glycans from rhASA.

*Dephosphorylation*—One milligram of rhASA was dialyzed against 150 mM NaCl/10 mM Tris-HCl (pH 8.0)/10 mM MgCl<sub>2</sub> and incubated with 20 milliunits of alkaline phosphatase from *E. coli* (Sigma-Aldrich) in a total volume of 1 ml for 4 h at 25 °C. Dephosphorylation was verified by measurement of the Man-6-P-dependent endocytosis of BHK cells. Endocytosis of the

dephosphorylated protein was reduced by >99%, indicating a complete loss of the Man-6-P residues.

**Desialylation**—One milligram of rhASA was dialyzed against 150 mM NaCl/20 mM sodium acetate (pH 5.5)/4 mM CaCl<sub>2</sub> and incubated with 50 milliunits of sialidase from *Vibrio cholerae* (Roche Applied Science) in a total volume of 1 ml for 24 h at 37 °C. Desialylation of rhASA was monitored by alterations in the isoelectric focusing pattern. As expected due to the low content of complex type *N*-glycans (11), <10% of the protein was modified. Subsequent to deglycosylation, dephosphorylation, or desialylation, the modifying enzyme (Endo H<sub>p</sub>, 70 kDa; alkaline phosphatase, 89 kDa; sialidase, 83 kDa) were separated from rhASA octamers (~460 kDa) by gel-filtration chromatography, taking advantage of the octamerization of ASA at acidic pH (15). For gel filtration, a Superdex 200 HR 10/30 column connected to an Äkta FPLC system (GE Healthcare Europe) and 150 mM NaCl/20 mM sodium acetate (pH 5.0) as mobile phase was used. Eluate fractions were concentrated and rebuffered to TBS (pH 7.3) in Centricon YM-10 centrifugal filter devices (Millipore, Schwalbach, Germany). Unmodified rhASA used as control was treated identically, but in the absence of the respective modifying enzyme.

#### Chemical Modification of rhASA

Exposed carbohydrates of rhASA were inactivated by sodium metaperiodate treatment (17). One milligram of rhASA was incubated with a final concentration of 10 mM sodium metaperiodate in 100 mM NaCl/20 mM sodium phosphate (pH 6.0) for 30 min at 20 °C. The reaction was stopped by the addition of 200 mM ethylene glycol and dialyzed overnight at 4 °C against 100 mM NaCl/20 mM sodium phosphate (pH 6.0). To reduce reactive aldehyde groups, sodium borohydrate was added to the dialysate to a final concentration of 100 mM. The mixture was incubated overnight at 4 °C and dialyzed extensively against TBS (pH 7.3). Under these conditions, 78% of the ASA activity was lost, but the immune reactivity was preserved.

#### Polycations

Poly-L-lysine (molecular mass, 1–5 kDa), unfractionated whole histone from calf thymus (molecular mass, 11.3–21.5 kDa), polybrene (hexadimethrine bromide), and BSA were from Sigma-Aldrich. BSA was cationized to pI 8–9 by carbodiimide-mediated amidation at pH 7.8 using hexamethylene-diamine (16).

## RESULTS

**Characterization of BBB Model**—An established cell culture model of the BBB consisting of primary PBCECs was used throughout this study (9, 10). The cells were cultured on micro-porous cell culture inserts, which were inserted into wells of 12-well plates to build up a two-chamber system (Fig. 1A). After confluency, the endothelial cell monolayer separates the apical from the basolateral compartment representing the blood and brain side of the capillary endothelium, respectively. The porcine BBB model is characterized by a high TEER, which is in the physiological range (1000 ohms × cm<sup>2</sup>) (Fig. 1B) and correspondingly, by a low apical-to-basolateral transfer of [<sup>14</sup>C]sucrose (permeability coefficient, 1.03 × 10<sup>-7</sup> cm/sec) and FITC

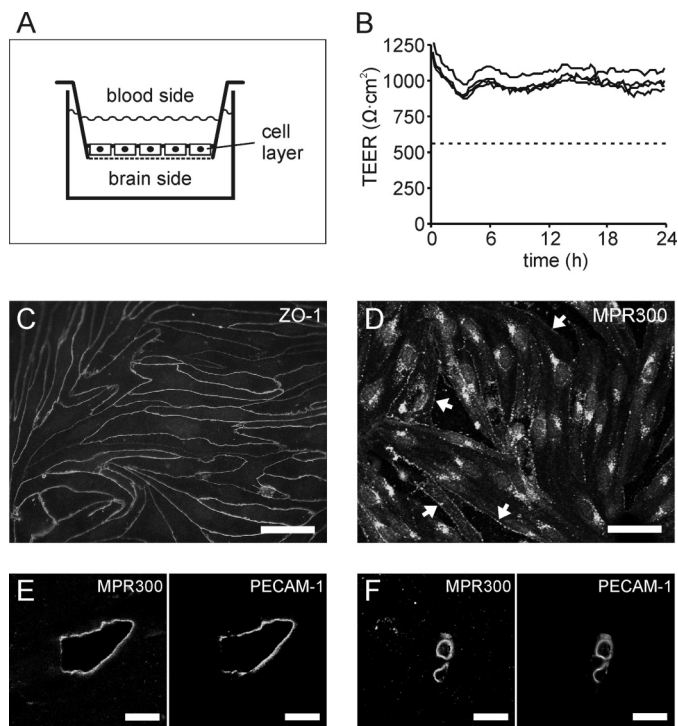


**FIGURE 1. Cell culture model of the blood-brain barrier.** A, a monolayer of PBCECs grown on Transwell filter inserts separates an apical and basolateral compartment representing the blood and brain side of the capillary endothelium, respectively. B, examples for continuous TEER measurements over 24 h. TEERs ranging ~1000 ohms × cm<sup>2</sup> are indicative of an intact barrier function. In all rhASA transfer experiments, wells with TEER values dropping below 600 ohms × cm<sup>2</sup> (dashed line) were excluded from the statistical evaluation. C, immunostaining of confluent PBCECs with antibody against ZO-1. D, immunostaining of subconfluent PBCECs with antibody against MPR300. Surface expression appears highest in fully spread cell flanks before they contact neighboring cells (arrows), possibly due to preferential sorting of MPR300 to membrane domains, which lie outside the focal plane after differentiation of the monolayer. E and F, co-immunostaining of sections through adult pig brain with antibodies against PECAM1 and MPR300 demonstrating MPR300 expression in endothelial cells of larger brain vessels (E) and brain capillaries (F). Scale bars represent 50 μm (C and D) and 10 μm (E and F), respectively.

dextran (70 kDa, permeability coefficient 7.63 × 10<sup>-9</sup> cm/sec). Thus, this model closely represents the *in vivo* situation. Moreover, as shown by time-dependent TEER measurements, the barrier properties are maintained for at least 24 h (Fig. 1B). Immunofluorescence staining of ZO-1 (zonula occludens-1 protein) of confluent monolayers revealed intense and delineated staining of all cell-cell contacts indicating well organized and fully developed tight junctions (Fig. 1C). To further characterize the BBB culture model, cells were stained with antibodies to MPR300. Signals were detectable on the cell surface and within intracellular compartments (Fig. 1D). The cellular distribution is in accordance with the known function of MPR300 as an endocytic receptor cycling between the plasma membrane, the endosomal compartment, and the trans-Golgi network (5). As a control, histological sections through adult pig brain were immunostained with anti-MPR300 antibodies. Co-immunostaining of the endothelial marker protein PECAM1 revealed high levels of MPR300 in endothelial cells of brain capillaries and larger brain vessels (Fig. 1, E and F). This excludes the possibility that the high receptor levels of PBCECs were due to an induction of the MPR300 expression under cell culture conditions.

## ASA Transport across the BBB

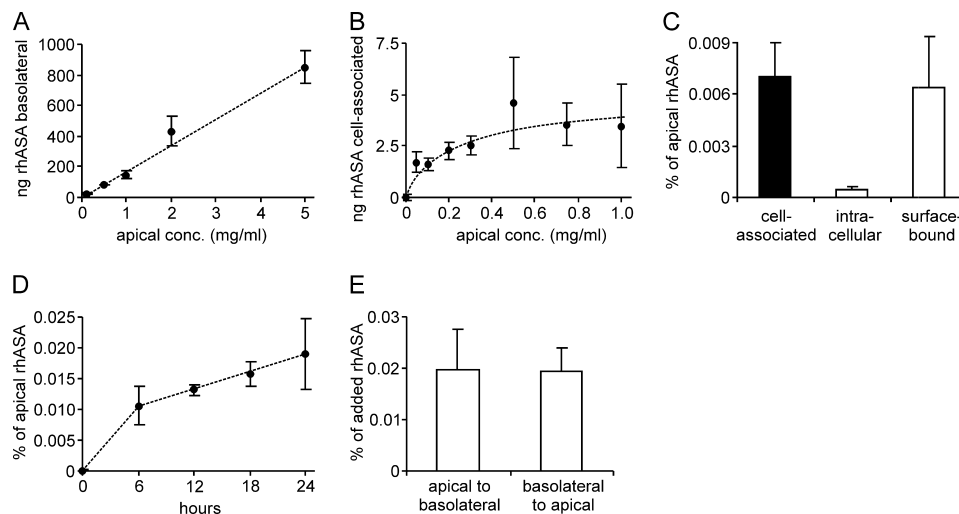


**FIGURE 2. Sorting of rhASA by PBCECs.** Basolateral (A) and cell-associated (B) rhASA levels were measured 24 h after addition of increasing concentrations (*conc.*) of rhASA to the apical medium. C, cell-associated, surface-bound, and intracellular rhASA levels were determined 24 h after addition of 0.1 mg/ml rhASA to the apical medium. D, time profile of basolateral transfer after addition of 0.1 mg/ml to the apical medium. E, transendothelial transfer after addition of 0.1 mg/ml rhASA either to the apical or to the basolateral medium. After 24 h, the total amount of rhASA was measured in the basolateral and apical medium, respectively, and normalized on the rhASA level in the contralateral compartment. Data shown in A–E represent means  $\pm$  S.D. of  $n = 3$ –5 wells per condition.

**Transport Measurements**—In the first set of experiments, increasing amounts of rhASA were added to the apical compartment. Basolateral concentrations were determined, and a linear increase of rhASA was found with increasing apical concentrations. Up to 5 mg/ml rhASA, no saturation could be detected (Fig. 2A). Higher rhASA concentrations induced a rapid breakdown of the TEER and barrier function and could therefore not be used (data not shown). Independent of the apical concentration,  $\sim 0.02\%$  of the total apical rhASA could be recovered from the basolateral compartment after 24 h. The amount of cell-associated rhASA was determined after repeated washing of the Transwell filters with  $1 \times$  PBS (pH 7.4). In contrast to the basolateral transfer, the amount of cell-associated rhASA became saturated when apical concentrations approached 1 mg/ml (Fig. 2B). To differentiate between internalized and surface-bound rhASA, cells incubated with 0.1 mg/ml rhASA for 24 h were washed with 50 mM glycine, 150 mM NaCl (pH 3.0). Compared with cells washed with  $1 \times$  PBS (pH 7.4) alone, the additional acidic wash removed  $\sim 90\%$  of the rhASA, indicating that only 10% of the cell-associated rhASA was internalized (Fig. 2C). The time profile of basolateral transfer indicates a constant transfer rate 6 to 24 h after addition of rhASA (Fig. 2D). In the first 6 h, the rate is higher, possibly due to the concomitant transient decline of the TEER that was consistently observed immediately after addition of rhASA to the apical medium (see Fig. 1B). To test for a possible active transfer process, rhASA was added in equal concentrations both to the apical and the basolateral medium. No change in the ratio between the rhASA concentrations was detectable within 24 h (data not shown). Furthermore, if minor imbalances in the apical-to-basolateral concentration ratios were applied, the concentration differences leveled out within 24 h, and values stabilized at  $\sim 1$  (data not shown). When rhASA was added to the basolateral compartment, a reverse transfer into the apical medium could be observed (Fig. 2E). The basolateral-to-apical and apical-to-basolateral transfer rates were indistinguishable. Lack of saturability, failure to accumulate in one compartment,

**TABLE 1**

Global analysis of *N*-glycans isolated from rhASA fractions separated by anion exchange chromatography. rhASA was bound to a Source 30Q anion exchange column and eluted with increasing NaCl concentrations. Fraction 1 contains the first eluting and least charged rhASA molecules. The concentration of the indicated monosaccharides is given as mol/mol rhASA. The total carbohydrate content of the five fractions ranged between 8.9 and 11.0% (data not shown). Neu5Ac, *N*-acetylneuraminic acid; GlcNAc, *N*-acetylglucosamine; GalNAc, *N*-acetylgalactosamine; Gal, galactose; Man, mannose; Man-6-P, mannose 6-phosphate; Fuc, fucose

Fraction	Neu5Ac	GlcNAc	GalNAc	Gal	Man	Man-6-P	Fuc
1	0.9	7.1	0.05	1.7	12.8	2.1	1.0
2	1.1	7.7	0.05	1.9	14.3	3.0	1.2
3	1.2	7.8	0.05	1.9	14.5	3.6	1.2
4	1.4	8.1	0.05	2.0	15.0	4.2	1.2
5	1.3	6.3	0.05	1.7	13.7	4.0	1.0

and bidirectional transport along the concentration gradient indicated that the transendothelial rhASA transfer is a passive transfer process.

**Charge-dependent Transfer Rates**—Passive transfer of substances across an endothelial cell layer might follow paracellular and/or transcellular routes. Passive transcellular transport depends on the adsorption of the molecule to the cell surface, its uptake, and its release at the opposite surface. Because the cell surface is charged negatively, adsorption is disfavored by negative charges of the molecule. To analyze possible effects of charge on the transendothelial transfer, the rhASA preparation was fractionated by anion exchange chromatography. Fractionation is feasible because ASA is a glycoprotein harboring variable concentrations of negatively charged Man-6-P and sialic acid residues in its *N*-glycans (11). The composition of the charged residues of the different rhASA fractions is given in Table 1. Aliquots of rhASA fractions 1 to 5 were added at a concentration of 0.1 mg/ml to the apical medium. ASA of all fractions passed the PBCEC monolayer (Fig. 3A). The permeability rate varied, however, between the fractions. It was highest for fraction 1 (low amount of negatively charged monosaccharides) and lowest for fractions 4 and 5 (high amount of negatively charged monosaccharides) ( $p < 0.05$ ). Interestingly, the amount of cell-associated rhASA showed the opposite tend-

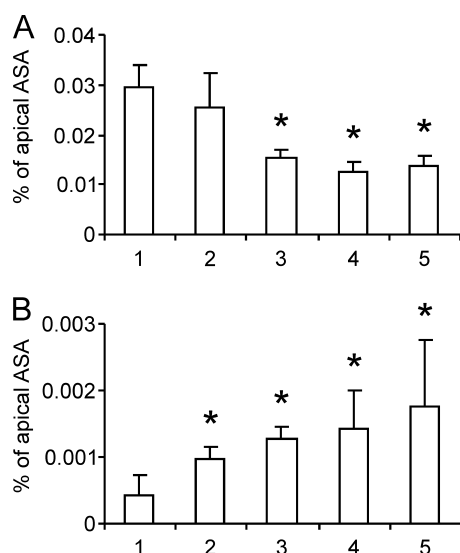


**FIGURE 3. Dependence of apical-to-basolateral transfer (A) and cell association of rhASA (B) from the rhASA charge.** Five fractions (1 to 5) of rhASA were separated by anion exchange chromatography and added at concentrations of 0.1 mg/ml to the apical medium of filter-plated PBCECs. Fractions 1 and 5 contained rhASA molecules with the least and most negatively charged *N*-glycans, respectively (see Table 1). Bars represent means  $\pm$  S.D. of  $n = 5$ –6 wells per condition. Asterisks indicate a statistically significant difference compared with fraction 1 (Student's *t* test,  $p < 0.05$ ).

ency, being >3-fold higher for fraction 5 compared with fraction 1 (Fig. 3B;  $p < 0.05$ ).

**Modification of *N*-Linked Oligosaccharides**—To analyze the significance of *N*-linked oligosaccharides for the apical-to-basolateral transfer in more detail, rhASA preparations with chemically or enzymatically modified *N*-glycans were tested. ASA has three *N*-linked glycosylation sites, all of which are glycosylated and carry predominantly high mannose type *N*-glycans (11). Therefore, the majority of the *N*-glycans could be removed by treatment with Endo H. Apical-to-basolateral transfer of deglycosylated rhASA was reduced by 51% (Fig. 4A;  $p < 0.05$ ). Sly and co-workers (17) have reported preclinical ERT studies in which periodate treatment of  $\beta$ -glucuronidase increased brain delivery of this lysosomal enzyme ~6-fold compared with untreated  $\beta$ -glucuronidase. Periodate oxidizes vicinal hydroxyl groups of terminal monosaccharides to aldehyde functions and dephosphorylates Man-6-P residues (19). To test possible effects of periodate treatment on the transendothelial rhASA transfer in our BBB *in vitro* system, rhASA was oxidized with 10 mM sodium metaperiodate for 30 min. SDS-PAGE did not reveal a size shift of the modified enzyme, confirming that the oligosaccharide side chains were not lost. In the transfer assay, the basolateral concentrations of periodate pretreated rhASA were reduced by 12% (Fig. 4A; not significant). We further tested the effect of dephosphorylation of rhASA with alkaline phosphatase, which, again neither reduced the ASA activity nor its migratory behavior in SDS-PAGE. When tested in the BBB cell culture model, apical-to-basolateral transfer of untreated and dephosphorylated rhASA was indistinguishable (Fig. 4A). To evaluate possible effects of sialic acids on transendothelial transfer rates, rhASA was treated with sialidase. Again, treatment did not alter the migration of rhASA in SDS-PAGE or its enzymatic activity. Treatment caused,

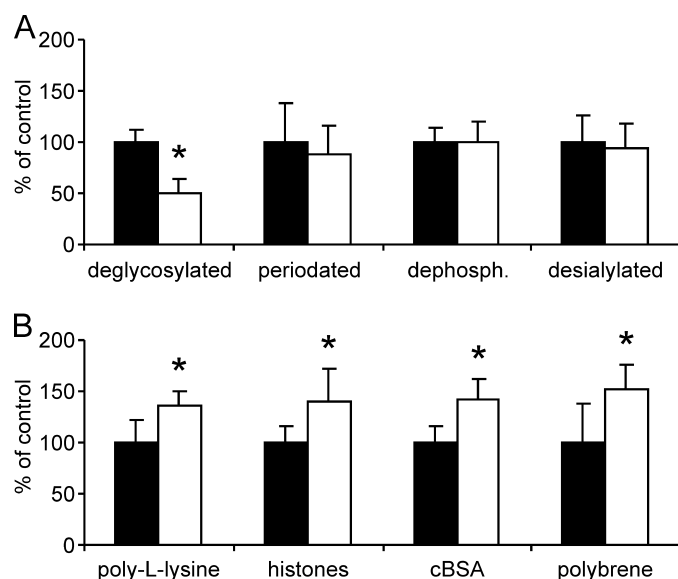


**FIGURE 4. Effects of chemical modifications (A) and polycations (B) on apical-to-basolateral transfer of rhASAs.** Basolateral rhASA levels measured 24 h after apical feeding of 0.1 mg/ml rhASA under modified conditions (open bars) are expressed as percent of controls, representing PBCECs incubated with unmodified rhASA and in the absence of polycations, respectively (filled bars). A, rhASA was modified as indicated by deglycosylation with Endo H, oxidation with periodate, dephosphorylation with alkaline phosphatase, or desialylation with sialidase. B, the indicated cations were added in a concentration of 5  $\mu$ M (poly-L-lysine, histones) and 0.2  $\mu$ M (cationized BSA (cBSA), polybrene), respectively. Bars represent means  $\pm$  S.D. of  $n = 3$ –11 wells per condition. Asterisks indicate statistically significant differences to controls (Student's *t* test,  $p < 0.05$ ).

however, a redistribution of protein bands with low pI values to bands with higher pI values after isoelectric focusing, indicating loss of negative charges from a given fraction of rhASA glycoproteins by desialylation. Apical-to-basolateral transfer of sialidase-treated rhASA was indiscernible from control rhASA (Fig. 4A).

**Effects of Polycations**—The inhibitory effect of negative charges of *N*-linked oligosaccharides might be explained by repulsive forces between the *N*-glycans of rhASA and the negatively charged surface of endothelial cells. Electrostatic repulsion might be reduced by partial neutralization of negative charges using molecules with multiple positive charges. To test this, we analyzed the impact of polycations on rhASA sorting. Poly-L-lysine, added in a concentration of 5  $\mu$ M (representing a ~5-fold molar excess to rhASA), promoted the apical-to-basolateral rhASA transfer by 36% compared with control samples (Fig. 4B;  $p < 0.05$ ). Higher poly-L-lysine concentrations of 25 or 100  $\mu$ M had no significant effect on transfer rates (data not shown). Histones added in a ~5-fold molar excess to rhASA increased the apical-to-basolateral rhASA transfer by 41% (Fig. 4B;  $p < 0.05$ ). Higher concentrations caused breakdown of the BBB. Cationized BSA added in a 1:5 molar ratio to rhASA increased the apical-to-basolateral transfer of rhASA by 42% (Fig. 4B;  $p < 0.05$ ). Higher cationized BSA concentrations (equimolar or 5-fold molar excess to rhASA) had no significant effect on rhASA transfer rates (data not shown). Polybrene added again in a 1:5 molar ratio to rhASA increased the measured basolateral rhASA concentrations by 51% (Fig. 4B;  $p < 0.05$ ). In summary, all four polycations, poly-L-lysine, cation-

## ASA Transport across the BBB

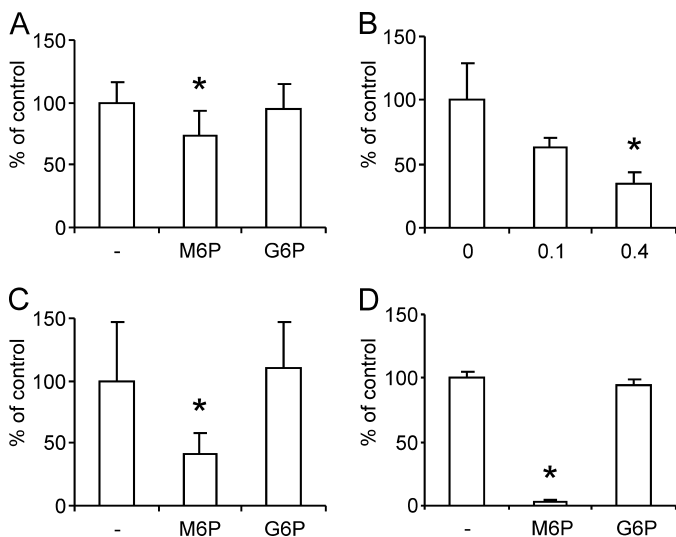


**FIGURE 5. Effects of Man-6-P on apical-to-basolateral transfer and cell association of rhASA.** *A*, PBCECs were incubated with rhASA (0.1 mg/ml) and either 7.5 mM glucose 6-phosphate (G6P), 7.5 mM mannose 6-phosphate (M6P) or no hexosyl phosphate (–). Basolateral rhASA levels were measured 24 h after feeding and are expressed as the mean percentage of control wells incubated without hexosyl phosphates.  $n = 9–13$  per condition. *B*, basalateral rhASA levels measured 24 h after incubation of PBCEC monolayers with 0.1 mg/ml rhASA and 0, 0.1, or 0.4 mg/ml  $\alpha$ -galactosidase A (GalA) as indicated ( $n = 3$  wells per condition). *C* and *D*, effect of 7.5 mM Man-6-P or 7.5 mM glucose 6-phosphate on the level of rhASA associated with PBCECs (*C*) and BHK cells (*D*), respectively. As a control, no hexosyl phosphate was added (–). Bars represent means  $\pm$  S.D. Asterisks indicate statistically significant differences to controls (Student's *t* test,  $p < 0.05$ ).

ized BSA, histones, and polybrene, increased the basolateral rhASA transfer by up to 40–50%.

**Competition with Man-6-P**—To test a possible contribution of Man-6-P receptors to the apical-to-basolateral transfer of rhASA, the MPR300 of the PBCECs was blocked competitively by addition of 7.5 mM Man-6-P, which represented a 2500-fold molar excess to Man-6-P residues of rhASA. Under these conditions, the apical-to-basolateral rhASA transfer was reduced by 27% on average (Fig. 5A;  $p < 0.05$ ). In contrast to Man-6-P, the Man-6-P epimer glucose 6-phosphate had no effect on basolateral rhASA concentrations. In a second experiment, competitive effects of the lysosomal enzyme  $\alpha$ -galactosidase A on the transendothelial rhASA transfer were investigated.  $\alpha$ -Galactosidase A has a Man-6-P content of 1.4 mol/mol (11) and was added in a concentration of 0.1 or 0.4 mg/ml. Consequently, the molar ratios between the Man-6-P residues of  $\alpha$ -galactosidase A and rhASA were around 1:2 and 2:1, respectively. Under these conditions, the apical-to-basolateral rhASA transfer rates were reduced by 39 and 65%, respectively (Fig. 5B;  $p < 0.05$  only for 0.4 mg/ml  $\alpha$ -galactosidase A). To measure effects of 7.5 mM Man-6-P on the level of cell-associated rhASA, PBCECs were compared with BHK cells. The binding/uptake by PBCECs could be only partially reduced by 59% (Fig. 5C;  $p < 0.05$ ), whereas binding/uptake by BHK cells was almost completely inhibited (Fig. 5D;  $p < 0.05$ ).

## DISCUSSION

ASA and other soluble lysosomal enzymes bear Man-6-P residues and bind to the insulin-like growth factor II/mannose 6-phosphate receptor MPR300 (5, 11, 18). Except for some

tumor cell lines, MPR300 is present on the plasma membrane of all cells analyzed so far. Also endothelial cells from adult pig brain express MPR300 (Fig. 1, D–F) and are capable to bind ASA in a Man-6-P-dependent manner. This has been demonstrated by competition experiments in which soluble Man-6-P reduced the amount of rhASA associated with PBCECs by 59% (Fig. 5C). Notably, binding and uptake of rhASA to other cell types such as BHK cells can be almost completely inhibited by Man-6-P (Fig. 5D). The cell type-specific difference in the residual binding capacity suggests that PBCECs, but not BHK cells, can interact with rhASA in a Man-6-P-independent manner. The net uptake of surface-bound rhASA by PBCECs is low. Only 10% of cell-associated rhASA is transported to intracellular compartments within 24 h (Fig. 2C).

Importantly, PBCECs do not only bind and internalize rhASA, but they also deliver significant amounts of enzyme to the basolateral medium. Around 8 ng of rhASA reach the basolateral compartment per mg of apical rhASA, per  $\text{cm}^2$  endothelial cell layer, and per h (Fig. 2A). Thus, the basolateral rhASA pool amounts to 0.02% of the apical pool over 24 h (Fig. 2E). The transendothelial transfer rate is low but provides an explanation for the unexpected effects of ERT on CNS storage in a metachromatic leukodystrophy mouse model. In these previous *in vivo* studies, injection of rhASA into the tail vein of adult ASA knock-out mice reduced sulfatide storage in the brain parenchyma (7, 8), challenging the generally accepted view that lysosomal enzymes cannot cross the BBB (4). Indeed, using capillary depletion,  $\sim 0.001\%$  of the totally administered enzyme could be detected in the brain parenchyma 1 h after injection of 20 mg/kg.<sup>4</sup> This amount can be estimated to represent  $\sim 10\%$  of the wild-type level. It is therefore likely that the low transfer rate seen in the BBB cell culture model (0.02% in 24 h) is of therapeutic relevance and reproduces the low transendothelial transfer rates seen in living mice.

In the BBB cell culture model, apical-to-basolateral transfer is not saturable up to high apical rhASA concentrations (Fig. 2A), and net movement of rhASA occurs only along its concentration gradient (Fig. 2E). Thus, an exclusively passive transfer process has to be taken into account. As could be concluded from our permeability measurements comparing rhASA and FITC-labeled dextran, the paracellular pathway may contribute to transendothelial transfer. On the other hand, the transfer rate of rhASA is influenced by enzyme charge modifications. Deglycosylation or high concentrations of negatively charged monosaccharides in the *N*-glycans, for example, reduce apical-to-basolateral transfer (Figs. 3A and 4A). Conversely, low concentrations of Man-6-P or sialic acids as well as addition of polycations increase the transfer rates (Figs. 3A and 4B). The susceptibility of transfer rates to these factors excludes simple paracellular leakage as a major pathway but clearly argues for a transcellular transport process. This conclusion is supported by the sustained high TEER of the system (Fig. 1B).

ASA is an enzyme with a low pI and therefore carries a net negative charge at neutral pH (6). It is striking that all factors or conditions, which promote apical-to-basolateral transfer, reduce the negative net charge of rhASA (polycations, low content of Man-6-P and sialic acids) and vice versa. Also, the inhibitory effect of deglycosylation (Fig. 4A) can be explained in this

manner because cleavage of the *N*-glycans may expose negatively charged carboxyl groups previously covered by the oligosaccharides. The impact of charge on the transendothelial transfer rate is a hallmark of adsorptive transcytosis (20). This pathway involves adsorption of a compound to the endothelial surface, a process which is disfavored by the repulsive forces between the negatively charged membrane and negative surface charges of the compound. As first described for albumin and immunoglobulins by Pardridge and co-workers (16, 22), the coupling of positively charged groups is, therefore, a means to increase adsorptive-mediated transcytosis of polypeptides across the BBB. Our *in vitro* data strongly suggest that cationization of rhASA might be an option in future preclinical trials to improve CNS delivery of enzymatic activity as well. However, such *in vivo* studies also have to take into account that cationic compounds may have adverse side effects. The cationic antibiotic gentamicin, for example, is nephrotoxic because it accumulates in lysosomes of proximal tubular cells and interferes with lysosomal function and membrane trafficking (23, 24). These effects have been partially ascribed to the strong electrostatic binding of the compound to anionic phospholipids of the inner surface of endosomal membranes inhibiting fusion with endocytic vesicles and lysosomes (25, 26).

Notably, the basolateral transfer of rhASA is not only affected by polycations but also by soluble Man-6-P, which diminishes apical-to-basolateral transfer of rhASA by a respectable 27% (Fig. 5A). This reduction might be explained by the anionic nature of Man-6-P, which may neutralize residual positive charges on the plasma membrane and/or rhASA, thereby further disfavoring adsorption. However, glucose 6-phosphate used as a control has the same charge, but no inhibitory effect (Fig. 5A). Therefore, the partial inhibition seen with Man-6-P must be charge-independent and specific to a blockade of the MPR300 pathway. Hence, MPR300 contributes to the basolateral sorting of rhASA. This conclusion is challenged by the observation that inactivation of Man-6-P-residues by periodate or dephosphorylation does not diminish the transfer rate (Fig. 4A). However, loss of Man-6-P-residues also reduces the negative net charge of rhASA, so that the lack of MPR300-dependent transcytosis may be outweighed by an increased rate of adsorptive transcytosis.

Taken together, our data suggest a model in which rhASA gets access to brain endothelial cells by two independent pathways, MPR300-mediated uptake and adsorptive endocytosis (Fig. 6). Although MPR300-dependent endocytosis leads to the engulfment of rhASA in clathrin-coated vesicles, rhASA taken up via adsorptive-mediated endocytosis may enter the cell also via caveolae (for a review, see Ref. 20). Caveolae may bud to form free vesicles that eventually fuse with the basolateral membrane. Clathrin-coated vesicles, on the contrary, may fuse, after loss of their clathrin coats, with endosomes. From there, rhASA may cross the cell and be delivered to the basolateral membrane.

Low pI and Man-6-P-residues are general features of soluble lysosomal enzymes, and our findings may therefore apply to other lysosomal polypeptides as well. Sly and co-workers (17, 27) have analyzed blood-to-brain transfer of the lysosomal enzyme  $\beta$ -glucuronidase in a mouse model of mucopolysac-

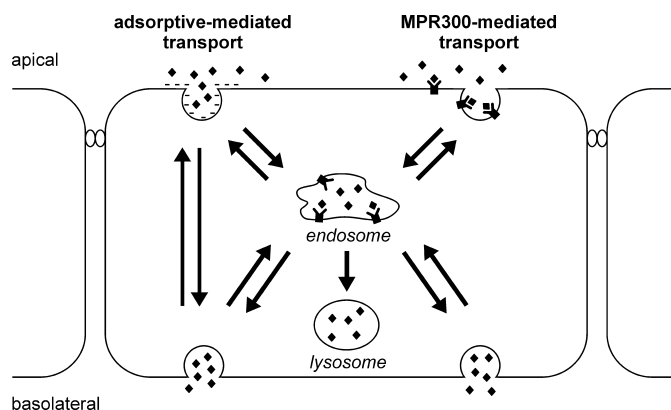


**FIGURE 6. Schematic representation of rhASA transport processes across the brain capillary endothelium.** Our data indicate that adsorptive endocytosis and MPR300-mediated internalization contribute to the transcytosis of rhASA (diamonds). MPR300 delivers soluble lysosomal enzymes in a clathrin-dependent manner to an endosomal compartment where acidification induces uncoupling of receptor and ligand (5, 18). The ligand subsequently can be sorted to the lysosome. In polarized PBCECs, the basolateral transfer of rhASA is reduced by Man-6-P, indicating that a fraction of endosomal rhASA is transported to the basolateral membrane and exocytosed. As suggested for other polypeptides, the adsorptive-mediated pathway of rhASA might involve clathrin-dependent transport across the endosomal compartment and/or direct transport of transcytotic vesicles budding from caveolae (20).

charidosis type VII treated by ERT. The authors found that overexpression of MPR300 at the BBB increases cerebral  $\beta$ -glucuronidase levels and glycosaminoglycan clearance from brain cells (27). On the other hand, inactivation of Man-6-P-residues of  $\beta$ -glucuronidase by periodate treatment had the same effect (17). It was a so far unresolved issue as to why both activation and inactivation of MPR300-mediated endocytosis have the potential to improve transendothelial transfer of  $\beta$ -glucuronidase. Our model explains this apparent contradiction, as two processes, one of which is stimulated (MPR300-mediated transcytosis) and one of which is hampered by Man-6-P (adsorptive transcytosis), may contribute to basolateral sorting.

It is still unclear why therapeutically effective amounts of  $\beta$ -glucuronidase, arylsulfatase A, and three other lysosomal enzymes (aspartylglucosaminidase,  $\alpha$ -mannosidase, and iduronate 2-sulfatase) are able to enter the brain parenchyma, whereas other lysosomal enzymes are efficiently kept off the central nervous system (7, 8, 28–32). The active site of ASA lies within a positively charged surface domain remote from the *N*-glycans and the dimerization domain and is therefore exposed to the surrounding (33). It is readily conceivable that this architecture has evolved to facilitate the interaction of ASA with the negatively charged sulfate residue of sulfatide. Notably, ASA is quite promiscuous and binds various sulfate-containing substrates including nonlipidic natural and artificial sulfate esters as well as phosphate and many other anions even at neutral pH (6, 34). This may explain why ASA also binds heparan sulfate leading to the attachment of extracellular ASA to surfaces of epithelial and endothelial cells under physiological conditions (35, 36). It might therefore be hypothesized that interaction of rhASA with sulfated glycosaminoglycans may concentrate the enzyme on the apical surface of brain endothelial cells and favor internalization via adsorptive or Man-6-P-dependent endocytosis. Binding to heparan sulfate has also been proposed to trigger the efficient cellular uptake of guanidi-

nylated neomycin or the protein transduction domain of the trans-activator of transcription (TAT) protein of the human immunodeficiency virus (21, 37).

In summary, rhASA penetrates PBCECs via two different transcellular passive transport processes, which depend on the surface charge of rhASA (adsorptive transcytosis) and the presence of Man-6-P-residues (MPR300-mediated transcytosis), respectively. Although MPR300-mediated transcytosis is favored by an increase of the Man-6-P content of the enzyme, adsorptive transcytosis is promoted by diminution of negative surface charges of rhASA. Cationization of rhASA and/or elevation of its Man-6-P-content may therefore be means to improve central nervous system delivery. Binding of ASA to sulfate residues of glycosaminoglycans exposed on the apical surfaces of brain endothelial cells may be causative for the observed transendothelial transport and the unexpected central nervous system effects detected in previous preclinical ERT studies.

### REFERENCES

- Greiner-Tollersrud, O. K., and Berg, T. (2005) in *Lysosomes* (Saftig, P., ed.) 1st Ed., pp. 60–73, Landes Bioscience, Georgetown, TX
- Meikle, P. J., Hopwood, J. J., Clague, A. E., and Carey, W. F. (1999) *JAMA* **281**, 249–254
- Desnick, R. J., and Schuchman, E. H. (2002) *Nat. Rev. Genet.* **3**, 954–966
- Beck, M. (2010) *IUBMB Life* **62**, 33–40
- Storch, S., and Braulke, T. (2005) in *Lysosomes* (Saftig, P., ed.) 1st Ed., pp. 17–26, Landes Bioscience, Georgetown, TX
- von Figura, K., Gieselmann, V., and Jaeken, J. (2001) in *The Metabolic and Molecular Bases of Inherited Disease* (Scriver, C. R., Beaudet, A. L., Sly, W. S., Valle, D., Childs, B., Kinzler, K. W., Vogelstein, B., eds.) pp. 3695–3724, McGraw-Hill, New York
- Matzner, U., Herbst, E., Hedayati, K. K., Lüllmann-Rauch, R., Wessig, C., Schröder, S., Eistrup, C., Möller, C., Fogh, J., and Gieselmann, V. (2005) *Hum. Mol. Genet.* **14**, 1139–1152
- Matzner, U., Lüllmann-Rauch, R., Stroobants, S., Andersson, C., Weigelt, C., Eistrup, C., Fogh, J., D'Hooge, R., and Gieselmann, V. (2009) *Mol. Ther.* **17**, 600–606
- Franke, H., Galla, H., and Beuckmann, C. T. (2000) *Brain Res. Brain Res. Protoc.* **5**, 248–256
- von Wedel-Parlow, M., Wölte, P., and Galla, H. J. (2009) *J. Neurochem.* **111**, 111–118
- Schröder, S., Matthes, F., Hyden, P., Andersson, C., Fogh, J., Müller-Loenies, S., Braulke, T., Gieselmann, V., and Matzner, U. (2010) *Glycobiology* **20**, 248–259
- Lischper, M., Beuck, S., Thanabalasundaram, G., Pieper, C., and Galla, H. J. (2010) *Brain Res.* **1326**, 114–127
- Baum, H., Dodgson, K. S., and Spencer, B. (1959) *Clin. Chim. Acta.* **4**, 453–455
- Matzner, U., Habetha, M., and Gieselmann, V. (2000) *Gene Ther.* **7**, 805–812
- Vagedes, P., Saenger, W., and Knapp, E. W. (2002) *Biophys. J.* **83**, 3066–3078
- Kumagai, A. K., Eisenberg, J. B., and Partridge, W. M. (1987) *J. Biol. Chem.* **262**, 15214–15219
- Grubb, J. H., Vogler, C., Levy, B., Galvin, N., Tan, Y., and Sly, W. S. (2008) *Proc. Natl. Acad. Sci. U.S.A.* **105**, 2616–2621
- Pohl, S., Marschner, K., Storch, S., and Braulke, T. (2009) *Biol. Chem.* **390**, 521–527
- Spiro, R. G. (1966) in *Methods in Enzymology* (Neufeld, E. F., and Ginsburg, V., eds) Vol. 8, pp. 26–52, Academic Press, New York, NY
- Hervé, F., Ghinea, N., and Scherrmann, J. M. (2008) *AAPS J.* **10**, 455–472
- Sarrazin, S., Wilson, B., Sly, W. S., Tor, Y., and Esko, J. D. (2010) *Mol. Ther.* **18**, 1268–1274
- Triguero, D., Buciak, J. B., Yang, J., and Partridge, W. M. (1989) *Proc. Natl. Acad. Sci. U.S.A.* **86**, 4761–4765
- Silverblatt, F. J., and Kuehn, C. (1979) *Kidney Int.* **15**, 335–345
- Skopicki, H. A., Zikos, D., Sukowski, E. J., Fisher, K. A., and Peterson, D. R. (1996) *Am. J. Physiol.* **270**, F531–F538
- Giurgea-Marion, L., Toubeau, G., Laurent, G., Heuson-Stiennon, J. A., and Tulkens, P. M. (1986) *Toxicol. Appl. Pharmacol.* **86**, 271–285
- Sorribas, V., Halaihel, N., Puttapparthi, K., Rogers, T., Cronin, R. E., Alcalde, A. I., Aramayona, J., Sarasa, M., Wang, H., Wilson, P., Zajicek, H., and Levi, M. (2001) *Kidney Int.* **59**, 1024–1036
- Urayama, A., Grubb, J. H., Banks, W. A., and Sly, W. S. (2007) *Proc. Natl. Acad. Sci. U.S.A.* **104**, 12873–12878
- Vogler, C., Levy, B., Grubb, J. H., Galvin, N., Tan, Y., Kakkis, E., Pavloff, N., and Sly, W. S. (2005) *Proc. Natl. Acad. Sci. U.S.A.* **102**, 14777–14782
- Dunder, U., Kaartinen, V., Valtonen, P., Väänänen, E., Kosma, V. M., Heisterkamp, N., Groffen, J., and Mononen, I. (2000) *FASEB J.* **14**, 361–367
- Roces, D. P., Lüllmann-Rauch, R., Peng, J., Balducci, C., Andersson, C., Tollersrud, O., Fogh, J., Orlacchio, A., Beccari, T., Saftig, P., and von Figura, K. (2004) *Hum. Mol. Genet.* **13**, 1979–1988
- Blanz, J., Stroobants, S., Lüllmann-Rauch, R., Morelle, W., Lüdemann, M., D'Hooge, R., Reuterwall, H., Michalski, J. C., Fogh, J., Andersson, C., and Saftig, P. (2008) *Hum. Mol. Genet.* **17**, 3437–3445
- Polito, V. A., and Cosma, M. P. (2009) *Am. J. Hum. Genet.* **85**, 296–301
- Lukatela, G., Krauss, N., Theis, K., Selmer, T., Gieselmann, V., von Figura, K., and Saenger, W. (1998) *Biochemistry* **37**, 3654–3664
- Stevens, R. L., Fluharty, A. L., Skokut, M. H., and Kihara, H. (1975) *J. Biol. Chem.* **250**, 2495–2501
- Mitsunaga-Nakatsubo, K., Akimoto, Y., Kawakami, H., and Akasaka, K. (2009a) *Dev. Genes. Evol.* **219**, 281–288
- Mitsunaga-Nakatsubo, K., Kusunoki, S., Kawakami, H., Akasaka, K., and Akimoto, Y. (2009b) *Med. Mol. Morphol.* **42**, 63–69
- Poon, G. M., and Gariépy, J. (2007) *Biochem. Soc. Trans.* **35**, 788–793